TMX #

NASA TECHNICAL MEMORANDUM

NASA TM X-64961

MÖSSBAUER STUDIES IN $Zn^{2+}_{0.3}\,Mn^{2+}_{0.7}\,Mn^{3+}_{y}\,Fe^{3+}_{2-y}\,O_4$

R. G. Gupta, R. G. Mendiratta,
and W. T. Escue
Electronics and Control Laboratory

August 1975

NASA

George C. Marshall Space Flight Center
Marshall Space Flight Center, Alabama

TECHNICAL REPORT STANDARD TITLE

1. REPORT NO.	2. GOVERNMENT ACCESSION NO.	3. RECIPIENT'S CATALOG NO.
NASA TM X-64961		

4. TITLE AND SUBTITLE	5. REPORT DATE
Mössbauer Studies in $Zn^{2+}_{0.3}\ Mn^{2+}_{0.7}\ Mn^{3+}_{y}\ Fe^{3+}_{2-y}\ O_4$	August 1975
	6. PERFORMING ORGANIZATION CODE
7. AUTHOR(S)	8. PERFORMING ORGANIZATION REPORT #
R. G. Gupta,* R. G. Mendiratta,* and W. T. Escue	
9. PERFORMING ORGANIZATION NAME AND ADDRESS	10. WORK UNIT NO.
George C. Marshall Space Flight Center Marshall Space Flight Center, Alabama 35812	11. CONTRACT OR GRANT NO.
	13. TYPE OF REPORT & PERIOD COVERED
12. SPONSORING AGENCY NAME AND ADDRESS	Technical Memorandum
National Aeronautics and Space Administration Washington, D. C. 20546	14. SPONSORING AGENCY CODE

15. SUPPLEMENTARY NOTES

*Department of Physics, Indian Institute of Technology, Hauz Khas, New Delhi-110029, India.
Prepared by Electronics and Control Laboratory, Science and Engineering.

16. ABSTRACT

The Mössbauer effect has proven to be very effective in the study of nuclear hyperfine interactions. The purpose of this report is to prepare and study ferrite systems having the formula $Zn^{2+}_{0.3}\ Mn^{2+}_{0.7}\ Mn^{3+}_{y}\ Fe^{3+}_{2-y}\ O_4$. These systems can be interpreted as manganese-doped zinc and a part of iron ions. A systematic study of these systems is presented in this report to promote better understanding of their microstructure for which various theories have been proposed.

17. KEY WORDS	18. DISTRIBUTION STATEMENT
	Unclassified — Unlimited W. T. Escue

19. SECURITY CLASSIF. (of this report)	20. SECURITY CLASSIF. (of this page)	21. NO. OF PAGES	22. PRICE
Unclassified	Unclassified	32	NTIS

TABLE OF CONTENTS

LIST OF ILLUSTRATIONS

LIST OF TABLES

TECHNICAL MEMORANDUM X- 64961

MÖSSBAUER STUDIES IN $Zn^{2+}_{0.3}\ Mn^{2+}_{0.7}\ Mn^{3+}_{y}\ Fe^{3+}_{2-y}\ O_4$

INTRODUCTION

Ferrites, which are a broad class of complex magnetic oxides containing Fe^{3+} and other metal ions, are materials of technological importance. They have immense industrial use and their devices have applications in the outer space as well as in the telecommunication programs. These materials also have extensive use in nonreciprocal microwave devices, computer memory elements, high frequency transformers, and permanent magnets. The inverse ferrite with zinc impurity at the substitutional sites are among the more important subclasses of ferrites, in terms of commercial use. The interest in these "mixed ferrites" is primarily due to the substantial reduction in the Curie temperature, increase in room temperature permeability, and decrease in the coercive force.

As discussed in Reference 1, the Mössbauer effect has proven to be very effective in the study of nuclear hyperfine interactions. The purpose of this report is to prepare and study ferrite systems having the formula $Zn^{2+}_{0.3}\ Mn^{2+}_{0.7}\ Mn^{3+}_{y}\ Fe^{3+}_{2-y}\ O_4$. This system can be interpreted as manganese-doped zinc ferrite in which manganese ions replace a part of zinc and a part of iron ions. A systematic study of these systems is presented in this report with a view to understand better their microstructure for which various theories have been proposed.

A BRIEF REVIEW OF VARIOUS THEORIES

Before going into the various theories proposed for the ferrimagnetism in ferrites, the spin exchange interaction which is responsible for the magnetic properties of ferrites is discussed.

Exchange interaction is a purely quantum mechanical phenomenon and it is difficult to assign a simple classical picture to it. In quantum mechanics, an electron is completely defined by its wave function, Ψ, which depends upon its spatial coordinates $(\bar{\gamma})$ and its spin state, σ, such that

$$\Psi = \Psi(\gamma, \sigma) \quad .$$

If the spin orbit coupling is so small as to be negligible, one can separate the spatial and the spin parts of the function so that

$$\Psi = \psi(\bar{\gamma})\kappa(\sigma) \quad .$$

The knowledge of Ψ immediately gives total energy E of the system for

$$E = \int \Psi^* H \Psi \, dv \quad ,$$

where H is the Hamiltonian operator.

Let us consider the simple case of two electrons in a molecule. The Hamiltonian operator in the absence of spin orbit coupling for such a system is

$$H = \frac{1}{2}\nabla_1^2 + \frac{1}{2}\nabla_2^2 + V_{1,2} + V_1 + V_2 \quad ,$$

where V_1 and V_2 are the potential energy functions for the two electrons in the field of the atomic nucleus and $V_{1,2}$ is the potential energy function for the electrostatic interaction between the two electrons. If $\psi_1(\bar{\gamma}_1)$ and $\psi_2(\gamma_2)$ are the spatial wave functions for the two electrons, quantum mechanics requires that the spatial wave function describing the two-electron system be given by

$$\Phi = \psi_1(\bar{\gamma}_1)\psi_2(\bar{\gamma}_2) \quad . \qquad (1)$$

One can obtain the energy eigenvalues from the Schroedinger equation,

$$H\Phi = E\Phi \quad .$$

From quantum mechanical considerations there is, however, a serious objection against the validity of Φ as described by equation (1). Because of the term, $V_{1,2}$, appearing in the Hamiltonian which depends upon the distance, $r_{1,2}$, between the two electrons, the probability density, $|\Phi|^2$, is asymmetric in $\bar{r}_1$ and $\bar{r}_2$. This implies that the two electrons can be separately identified as number 1 and number 2, respectively. This is inadmissible because in quantum mechanics a continuous observation of the varying position of an electron is not possible without so interfering with the system that it no longer could be counted as isolated. It is not possible, therefore, to know which electron is observed in a measurement. All that can be said in a measurement is that an electron is at point $\bar{r}_1$ and another at the point $\bar{r}_2$. Quantum mechanics, therefore, requires that the square of the spatial wave function of the two electronics must be symmetric in $\bar{r}_1$ and $\bar{r}_2$, which implies that the wave function Φ used to describe the two electron system should be symmetric or antisymmetric on interchanging coordinates $\bar{r}_1$ and $\bar{r}_2$. There are only two ways of constructing such a wave function:

$$\Phi_s = \psi_1(r_1)\psi_2(r_2) + \psi_2(r_1)\psi_1(r_2) \quad ,$$

and (2)

$$\Phi_a = \psi_1(r_1)\psi_2(r_2) - \psi_2(r_1)\psi_1(r_2)$$

where the subscripts s and a on Φ represent symmetric and antisymmetric wave functions. If the wave functions described by equation (1) were used, the eigenvalues of the energy corresponding to the operator $V_{1,2}$ would be that of Coulomb interaction between the two electrons. The use of wave functions given by equation (2), however, gives the energy as a sum of two values: one corresponding to the Coulomb energy and the other which is commonly known as the exchange energy. The origin of exchange interaction energy is, therefore, based on the quantum mechanical requirement that the wave function describing the two electron system should either be symmetric or antisymmetric.

If one still wishes to retain the idea that an electron maintains its identity and, therefore, can be distinguished from another electron, it is necessary to assume that the electron undergoes very rapid and undetectable exchanges of states. Under this assumption, though the one electron state may be reasonably well defined, one cannot predict which electron occupies which state. Because of the exchange in the electronic states, the corresponding energy is given the name of exchange interaction energy.

Since the total wave function, which is the product of spatial and spin wave functions, has to be antisymmetrical for an electron (in fact for any fermion), a symmetrical spatial wave function requires an antisymmetric spin wave function and vice versa. The symmetry requirement on the wave function necessitates a special spin configuration and as a result it can be alternately said that the exchange energy is due to direct spin-spin interaction. It is for this reason that the term spin exchange interaction is often used to represent this phenomenon.

In a solid, the spin exchange interaction is confined not only to the electrons of the same ion but also to the electrons of the neighboring ions. This spin exchange interaction is a short range interaction and. therefore, is appreciable only for those electrons whose wave functions overlap. Clearly, this spin exchange interaction should be a function of interatomic distances in the solid. Detailed calculations [2] indicate that the spin exchange interaction is quantitatively given by a function J, called the spin exchange integral. The interaction energy E_{ex} between "i"th and "j"th electrons becomes

$$E_{ex} = -KJ\bar{S}_i \cdot \bar{S}_j \quad ,$$

where K is a constant and $\bar{S}_i$ and $\bar{S}_j$ are the spin of the two electrons.

When J is positive, the parallel orientation of neighboring spins is favored and the material is called ferromagnetic, e.g., Fe, Co, Ni, etc. In materials such as MnO, CoS, $MnAu_2$, NiF_2, CrF_3, etc. with the J being negative, antiparallel arrangement of neighboring atomic spins is more stable. Such materials are called antiferromagnetic materials.

A particular branch of antiferromagnetic materials is known as ferrimagnetics. If the spins of the neighboring atoms which are aligned in the opposite direction are not equal so that a perfect cancellation of their magnetic moment

does not occur, the material is called ferrimagnetic. Examples of such materials are $NiFe_2O_4$, $ZnFe_2O_4$, and $MnFe_2O_4$.

The metal-metal distances in ferrimagnetics are sufficiently large that the direct exchange interaction may be expected to be very weak. It is apparent that the strong antiferromagnetic interactions in such materials must somehow involve the participation of the intervening anions. In considering the case of two Fe^{3+} ions separated by an O^{2-} ion in ferrites, the outer shell of the anion in the ground state has the electronic configuration s^2p^6. The p-wave function overlaps the 3d bonding orbitals of the neighboring metal ions. This overlap makes it possible to cause a nonzero exchange interaction between the neighboring metal ions. This exchange interaction is often termed as super exchange interaction.

The details on which the super exchange interaction depends are the metal-metal distances and the angular distributions of the cations around the oxygen ions [3].

To decide the suitability of magnetic material for a particular application, it is necessary to have a good idea concerning the internal magnetic field. The internal magnetic field [3], H_n, at the nucleus can be expressed as

$$H_n = H_{Local} + H_D + H_O + H_c \quad ,$$

where H_{Local} is the local internal field, H_D is the dipolar field, H_O is the orbital current field, and H_c is the Fermi contact field.

As shown in Reference 3, since the internal magnetic field is proportional to the saturation magnetization in the sample, various theories proposed to explain the saturation magnetization are also applicable to the discussion of internal magnetic fields.

Neel [4] proposed that the existence of spinel structure is due to two interpenetrating sublattices A and B. In the A-sublattice, metal ions are proposed to be tetrahedrally coordinated to four oxygen ions whereas the metal ions of B-site are octahedrally coordinated to six oxygen ions. Further, the magnetic spins of the two sublattices were assumed to point in the opposite

directions. This theory could successfully explain the magnetic moment of many ferrites such as $MnFe_2O_4$, Fe_3O_4, $NiFe_2O_4$, etc. However, it cculd not explain the variation in the saturation magnetization when varying amounts of diamagnetic zinc were added to these ferrites.

Yafet and Kittel [5] explained the variation of saturation magnetization in zinc-doped ferrites to a limited extent. With magnetization M of the lattice being given by

$$M = M_B - M_A$$

where M_B and M_A are the magnetizations of B and A sublattices, respectively and since nonmagnetic zinc has the tendency to occupy the A-site [3], M_A decreases with increasing concentration of zinc. This explains the initial rise in M with increasing zinc concentration. The introduction of zinc also decreases the A-B interaction as felt by the B-ions without affecting the B-B interaction. When the zinc concentration becomes appreciable, the B-B interaction dominates and consequently the spins in the B-sublattice start to orient antiparallel to one another. At this point, the B-sublattice divides into two or more sublattices whose magnetizations are canted relative to each other. The resultant total B-sublattice magnetization,

$$M_B = \sum_i M_{Bi} \quad ,$$

remains antiparallel to M_A but is reduced in magnitude. The net magnetization, therefore, decreases. This theory could roughly explain the behavior of saturation magnetization with nonmagnetic Zn concentration within the limiting range of $0.3 \leq \kappa \leq 0.7$.

Kaplan [6] had suggested the possibility of spin canting of magnetic ions in the A-sublattice also. However, he could not explain quantitatively the observed variation of saturation magnetization with x.

Anderson [7] suggested that the canted structure would, at most, have a local order. Neel concluded that if the B-site ion has two or more iron ions on the A-site in the immediate neighborhood, the B-site iron is magnetized parallel to the average B-site magnetization. If, however, all the surrounding A-sites are occupied by nonmagnetic zinc ions, the B-B interaction will cause the B-ions spins to invert. It was further concluded that the exchange field at the B-site, due to one Fe^{3+} ion at the A-site, is almost cancelled by all the first B-site neighbors. This hypothesis gives qualitative agreement with the experimental magnetization curve. However, the curve falls off too rapidly with x above 0.5.

Gilleo [8] considered the local field model and assumed that the B-site ions with fewer than two magnetic ions on the A-sites do not participate in ferrimagnetism and are essentially paramagnetic. No justification, however, has been given for this assumption.

Nowik [9] recently obtained better quantitative agreement making a slightly different assumption concerning the number of zinc neighbors on A-sites necessary to cause spin inversion on a B-site. The number of Zn^{2+} neighbors on A-sites has been proposed to be different for different ferrites. The calculations were, however, made for 0 K and it appears difficult to make similar calculations at higher temperatures.

Ishikawa [10] suggested the existence of magnetically isolated clusters around which all the A-sites are occupied by zinc ions. These clusters do not participate in the A-B interaction with the other lattice and therefore behave like free particles. The main objection to this theory is regarding the formation probability of such clusters.

SAMPLE PREPARATION

The samples were prepared by the dry ceramic technique on the same lines as reported in Reference 1. Using the known molecular weights of starting oxides, appropriate quantities of various oxides were taken in accordance with the following solid reactions:

$$4MnO_2 \xrightarrow{800°C} 2Mn_2O_3 + O_2 \quad ,$$

$$2(1 - x)MnCO_3 + 2xZnO + yMn_2O_3 + (2 - y)Fe_2O_3$$

$$2Zn_x^{2+}Mn_{1-x}^{2+}Fe_{2-y}^{3+}Mn_y^{3+}O_4 + 2CO_2 + O_2 \quad .$$

The loss in weight of the product ferrite was equal tc the combined weight of oxygen and carbon dioxide lost during the reaction as calculated from the previous equations. This indicated that the reaction proceeded exactly as planned.

To ensure that the samples, so prepared, were exactly the ones intended to be studied, the following independent checks were made on the product samples:

1. X-ray powder diffraction
2. Quantitative chemical analysis
3. Saturation magnetization and Curie temperature measurements.

The details of all these methods are given in Reference 3. The results obtained from these tests strongly indicate that the preparation method of the desired ferrites is satisfactory.

EXPERIMENTAL PROCEDURE

A constant acceleration electromagnetic drive was used to record the Mössbauer spectra. Gamma rays were detected by a 1 mm thick NaI scintillation crystal coupled to a Harshaw photomultiplier tube. A thin beryllium window was used in front of NaI crystal to cut off 6.63 keV X-rays from ^{57}Co source. The pulses corresponding to the desired 14.4 keV energy were selected using a single channel analyzer and fed to a 400-multichannel analyzer operated in a time-sequenced storage mode.

The radioactive source preparation techniques and the procedure used to analyze the complex Mössbauer spectra by computer fit are given in detail in Reference 3.

RESULTS AND DISCUSSION

The Mössbauer spectra of $Mn^{2+}_{0.7}\ Zn^{2+}_{0.3}\ Fe^{3+}_{2-y}\ Mn^{3+}_{y}\ O_4$ with values of x varying from 0.0 to 1.0 in steps of 0.1 are shown in Figures 1 through 11. These room temperature Mössbauer spectra are the parabolic effect corrected spectra [1]. A standard sodium nitroprusside (SNP) Mössbauer spectrum was taken with each of these spectra for calibration purposes. The Mössbauer spectra given in Figures 1 through 4 show a six-line hyperfine Zeeman pattern. Attempts were made to fit 12 lines. However, best fit was obtained for only six lines indicating that the two sextets, one due to Fe^{3+} ions at the tetrahedral site and the other due to Fe^{3+} at the octahedral site, could not be resolved. The relaxation effects in the samples with y values up to 0.3 (Figs. 1 through 4) are not very large; thus, it is possible to identify the line positions with some degree of accuracy. The quadrupole splitting in these samples was calculated from the observed line positions using [11]

$$\Delta\theta = \frac{1}{4}\left(E_6 - E_5 - E_1 + E_2\right) \quad ,$$

where $(E_6 - E_5)$ is the separation between the fifth and sixth lines and $(E_1 - E_2)$ is the separation between the second and first lines. The value of quadrupole splitting for these samples having y values up to 0.3 was approximately 0.02 mm/s, which is very small. For calculating the internal hyperfine magnetic fields, the quadrupole splitting was, therefore, assumed to be negligible. The values of hyperfine fields are listed in Table 1. For these values of y it is evident that the internal hyperfine magnetic field gradually decreases as the concentration of Mn^{3+} increases. This can be explained as follows.

The ionic distribution at the tetrahedral and the octahedral sites for the sample $Mn^{2+}_{0.7}\ Zn^{2+}_{0.3}\ Fe^{3+}_{2}\ O_4$ can be written [3] as

$$\left(Zn^{2+}_{0.3}Mn^{2+}_{0.7-a}Fe^{3+}_{a}\right)\left[Mn^{2+}_{a}Fe^{3+}_{2-a}\right]O_4 \quad ,$$

TABLE 1. INTERNAL MAGNETIC FIELDS AND CORRELATION TIMES, τ_s, FOR SAMPLES

Absorber	Magnetic Field (kg)	Correlation Time, τ_s (mm/s)
$Mn_{0.7}Zn_{0.3}Fe_2O_4$	450.93 ± 2.62	2.65
$Mn^{2+}_{0.7}Zn^{2+}_{0.3}Mn^{3+}_{0.1}Fe^{3+}_{1.9}O_4$	430.72 ± 2.78	2.61
$Mn^{2+}_{0.7}Zn^{2+}_{0.3}Mn^{3+}_{0.2}Fe^{3+}_{1.8}O_4$	425.02 ± 3.09	2.57
$Mn^{2+}_{0.7}Zn^{2+}_{0.3}Mn^{3+}_{0.3}Fe^{3+}_{1.7}O_4$	397.62 ± 4.95	2.55
$Mn^{2+}_{0.7}Zn^{2+}_{0.3}Mn^{3+}_{0.4}Fe^{3+}_{1.6}O_4$	331.71 ± 12.38	-
$Mn^{2+}_{0.7}Zn^{2+}_{0.3}Mn^{3+}_{0.5}Fe^{3+}_{1.5}O_4$	294.13 ± 15.47	-
$Mn^{2+}_{0.7}Zn^{2+}_{0.3}Mn^{3+}_{0.6}Fe^{3+}_{1.4}O_4$	286.18 ± 8.66	-
$Mn^{2+}_{0.7}Zn^{2+}_{0.3}Mn^{3+}_{0.7}Fe^{3+}_{1.3}O_4$	281.45 ± 6.19	-

where the parentheses and the brackets represent tetrahedral and octahedral sites, respectively. From charge considerations it is apparent that any Mn^{3+} introduced will replace only Fe^{3+} ions. Since various samples with different Mn^{3+} concentrations were prepared in exactly the same manner, it is reasonable to expect that the value of a in this ion distribution formula is the same for all samples. When Mn^{3+} is introduced to replace Fe^{3+} ions, the following three different possibilities can occur:

1. Mn^{3+} ions go to replace tetrahedral Fe^{3+} ions.
2. Mn^{3+} ions go to replace octahedral Fe^{3+} ions.
3. Mn^{3+} ions partly replace the octahedral and partly the tetrahedral Fe^{3+} ions.

There is no possibility of Mn^{3+} going to the interstitial space for reasons discussed in Reference 3. In the case of first possibility in which Mn^{3+} ions go to tetrahedral Fe^{3+} sites, the ionic distribution formula can be expressed as

$$\left(Mn^{2+}_{0.7-a}Zn^{2+}_{0.3}Mn^{3+}_{z}Fe^{3+}_{a-z}\right)\left[Mn^{2+}_{a}Fe^{3+}_{2-a}\right]O_4 \quad .$$

The magnetic moment of Mn^{3+} is $4\mu_B$ whereas that of Fe^{3+} is $5\mu_B$. Assuming A-B interaction to be much stronger than A-A and B-B interactions, it is apparent that the magnetic moment of A-sublattice decreases as Mn^{3+} replaces Fe^{3+} at the A-site. This would weaken the A-B interaction experienced by the octahedral Fe^{3+} ions. Furthermore, the B-B interaction remains unchanged in this process. Since the magnetization of B-sublattice can be written as

$$M_B = M_{BA} - M_{BB}$$

where M_{BA} is the magnetization due to A-B interaction as experienced by the octahedral Fe^{3+} ions and M_{BB} is the magnetization due to B-B interaction experienced by the same octahedral Fe^{3+} ions, it is apparent that the magnetization of B-sublattice will decrease. The A-B interaction as seen by the tetrahedral Fe^{3+} ions remains unchanged whereas the A-A interaction as seen by the tetrahedral Fe^{3+} ions would decrease. Again, with the magnetization of A-sublattice given by

$$M_A = M_{AB} - M_{AA} \quad ,$$

the magnetization of A-sublattice increases. Since the net magnetization is the difference of M_B and M_A, it is clear that as Mn^{3+} replaces the tetrahedral Fe^{3+} ions, the magnetization and the internal hyperfine magnetic field must decrease.

If, however, Mn^{3+} replaces octahedral Fe^{3+} ion, the ionic distribution can be expressed as

$$\left(Mn^{2+}_{0.7-a}Zn^{2+}_{0.3}Fe^{3+}_{a}\right)\left[Mn^{2+}_{a}Mn^{3+}_{z}Fe^{3+}_{2-a-z}\right]O_4 \quad .$$

Proceeding on the arguments given in the preceding paragraph, it is easy to see that in this process the magnetization of B-sublattice increases whereas the magnetization of A-sublattice decreases as Mn^{3+} goes to substitute the octahedral Fe^{3+} ion. Consequently, the magnetization and the internal hyperfine magnetic field will increase.

Let us now consider the third possibility where Mn^{3+} ions partly replace the tetrahedral Fe^{3+} ions and partly the octahedral Fe^{3+} ions. The manganese going to a tetrahedral site would result in a decrease in the internal hyperfine magnetic field whereas Mn^{3+} going to an octahedral site would result in an increase in the internal hyperfine magnetic field. Furthermore, it is easy to see that the decrease in the hyperfine field due to Mn^{3+} replacing the tetrahedra iron ions is approximately the same as the increase in the hyperfine field when Mn^{3+} ions replace the octahedral iron ions. Since in the present work the net internal hyperfine magnetic field is observed to decrease gradually as y increases, it is apparent that only first and third possibilities are probable. That is, either the Mn^{3+} ions replace only the tetrahedral iron ion or they replace octahedral as well as tetrahedral iron ions. It is clear that if the second alternative holds true, the probability of Mn^{3+} replacing the tetrahedral iron ion is more than the probability of its replacing the octahedral iron ions.

The Mössbauer spectra for samples with y values between 0.4 to 0.7 (Figs. 5 through 8) indicate the presence of relaxation effects similar to those discussed in Reference 1 for A-samples with x values between 0.3 to 0.5.

With the line positions not being very distinct, it is impossible to draw any accurate quantitative conclusion concerning the internal hyperfine magnetic field and the relaxation times. However, a rough estimate of the internal hyperfine magnetic field was made from the position of the outer two lines. The observed values are given in Table 1. Because of large relaxation effects, these values are only approximate.

Relaxation phenomena are of two types: spin-spin relaxation and spin-lattice relaxation. The spin-spin relaxation is significant when the internal magnetic fields are strong. The strong magnetic bonds between the magnetic ions do not allow the spin inversion. There is, however, slight reorientation of the spin directions. In this process there is an exchange of energy between the spin and the internal magnetic field. If, however, the internal magnetic fields are weak, the magnetic bonding between the various magnetic ions are not very strong and the spins easily flip over. In this case there is a simultaneous creation of a lattice phonon of energy equal to the energy difference between the two spin orientations. Thus in this process there is an exchange of energy between the spin and the lattice. This type of relaxation phenomenon is called the spin-lattice relaxation.

The values of correlation time and spin flip flop frequency for samples with y values from 0.0 to 0.3 are listed in Table 1. Because of the uncertain line positions, it was not possible to calculate these parameters for other values of y. As is evident from Table 1, the decrease in the value of correlation time is fairly large around $y = 0.4$. This could be because of the presence of spin-lattice relaxation which becomes significant only when the internal hyperfine magnetic fields become weak (Table 1). The nature of these Mössbauer spectra (Figs. 5 through 8), which we attribute to the presence of spin-lattice relaxation, is similar to the nature of the Mössbauer spectra in the presence of spin-lattice relaxation as seen by earlier workers [12].

The Mössbauer spectra with y values from 0.8 to 1.0 as shown in Figures 9 through 11 indicate a clear quadrupole doublet. Attempts were made, without success, to fit more than two lines. The quadrupole splittings and the isomer shifts as observed from these spectra are shown in Table 2.

The doublet seen in these spectra is attributed to the Fe^{3+} ions at the B-site. For these large values of y one should expect only, if at all, a very small quantity of Fe^{3+} at the A-site. The Mössbauer signal due to Fe^{3+} at A-site would, therefore, be very weak and would be masked by the quadrupole

TABLE 2. ISOMER SHIFTS AND QUADRUPOLE SPLITTINGS FOR SAMPLES

Absorber	Isomer Shift[a] (mm/s)	Quadrupole Splitting (mm/s)
$Mn^{2+}_{0.7}Zn^{2+}_{0.3}Mn^{3+}_{0.8}Fe^{3+}_{1.2}O_4$	0.147 ± 0.006	1.024 ± 0.026
$Mn^{2+}_{0.7}Zn^{2+}_{0.3}Mn^{3+}_{0.9}Fe^{3+}_{1.1}O_4$	0.142 ± 0.006	0.889 ± 0.026
$Mn^{2+}_{0.7}Zn^{2+}_{0.3}Mn^{3+}_{1.0}Fe^{3+}_{1.0}O_4$	0.154 ± 0.006	0.999 ± 0.026

a. Isomer shifts are with respect to Cu source.

doublet due to Fe^{3+} at B-site. From Table 2 it is observed that there is no significant change in the quadrupole splitting when y changes from 0.8 to 1.0. This can be explained as being due to Mn^{3+} replacing Fe^{3+} at B-site rather than at the A-site. As previously explained, there is hardly any iron at A-site for these values of y. The replacement of Fe^{3+} (0.67 Å) by a bigger ion such as Mn^{3+} (0.70 Å) would expand the octahedron preserving the overall initial symmetry; therefore, one should not anticipate any significant change in the quadrupole splitting.

The justification for the large quadrupole splitting obtained for these samples as compared to those for A-samples is as follows. The introduction of Zn^{2+} in A-sublattice first increases the quadrupole splitting (which is due to the replacement of Mn^{2+} by Zn^{2+}) and beyond a certain concentration of Zn^{2+}, the quadrupole splitting decreases (this due to the replacement of Fe^{3+} by Zn^{2+} at A-site). In B-samples, however, because Mn^{3+} ions replace only Fe^{3+} ions at all concentrations of Mn^{3+}, it is apparent that the quadrupole splitting continues to increase with y. Unlike the case of A-samples there is no decrease of quadrupole splitting for higher concentrations of the dopant. The quadrupole splitting, therefore, has large values for larger values of y in these samples.

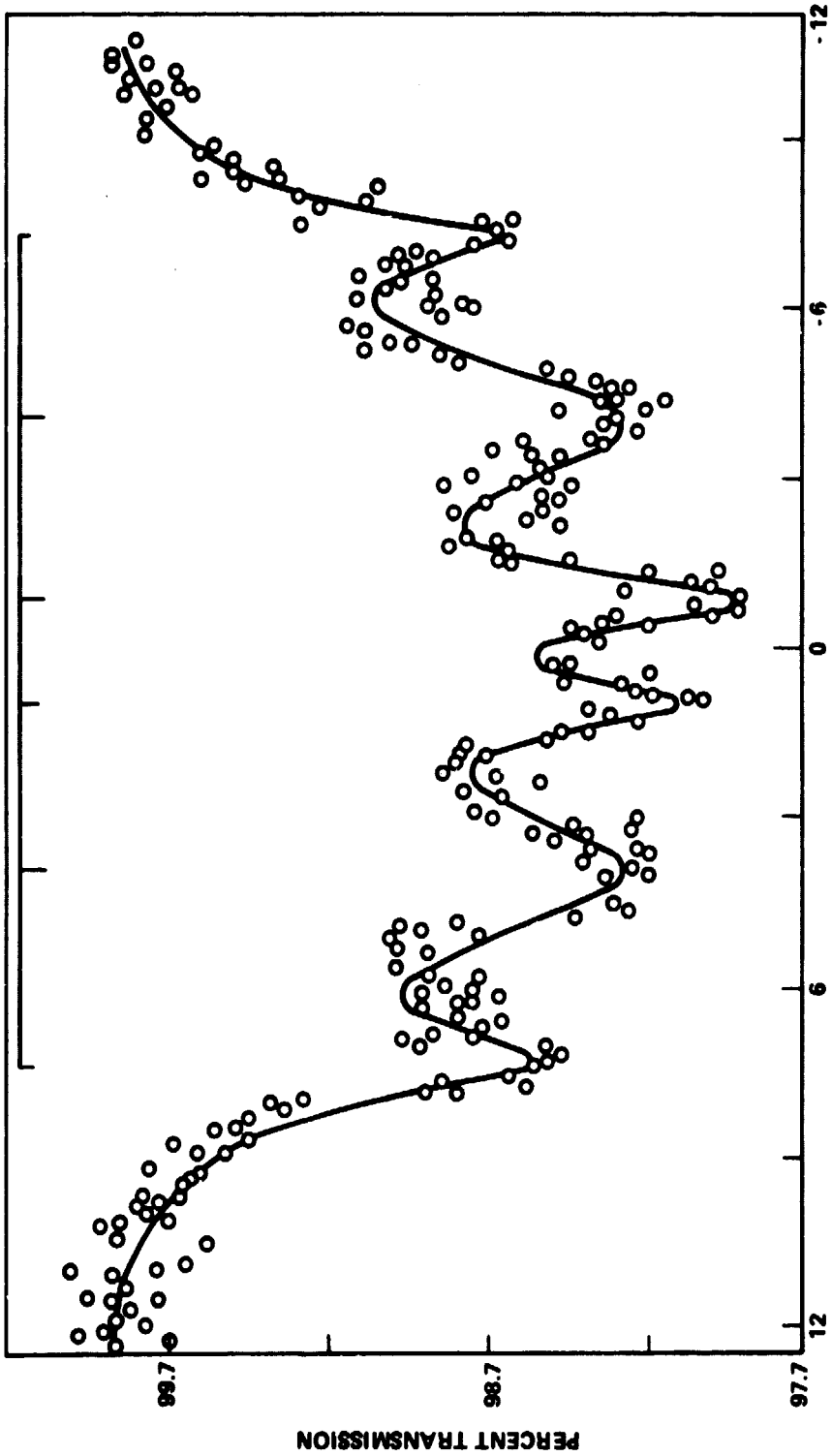

Figure 1. Mössbauer spectrum of $Zn^{2+}_{0.3}Mn^{2+}_{0.7}Fe^{3+}_{2}O_4$.

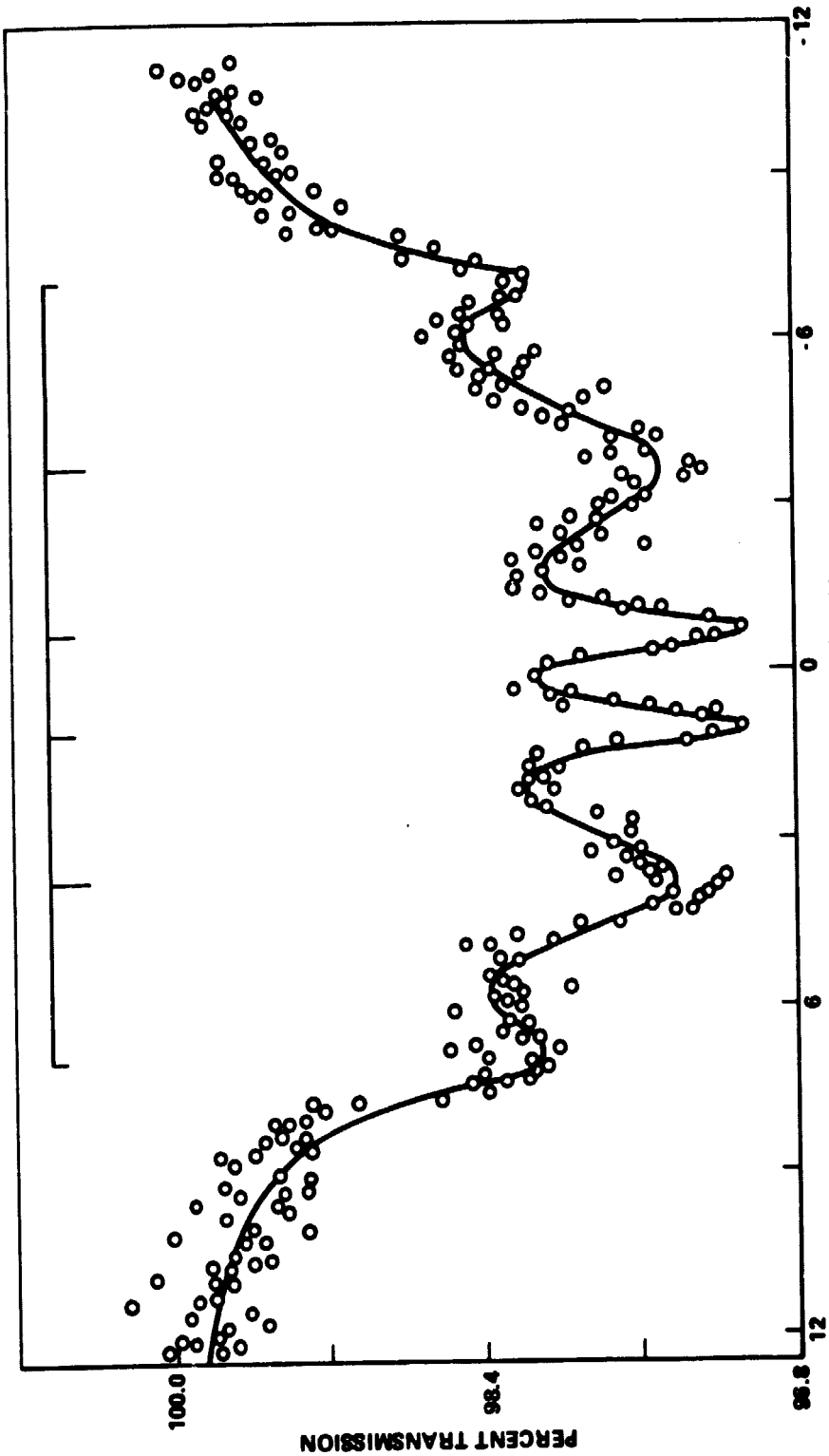

Figure 2. Mössbauer spectrum of $Zn^{2+}_{0.3}Mn^{2+}_{0.7}Mn^{3+}_{0.1}Fe^{3+}_{1.9}O_4$.

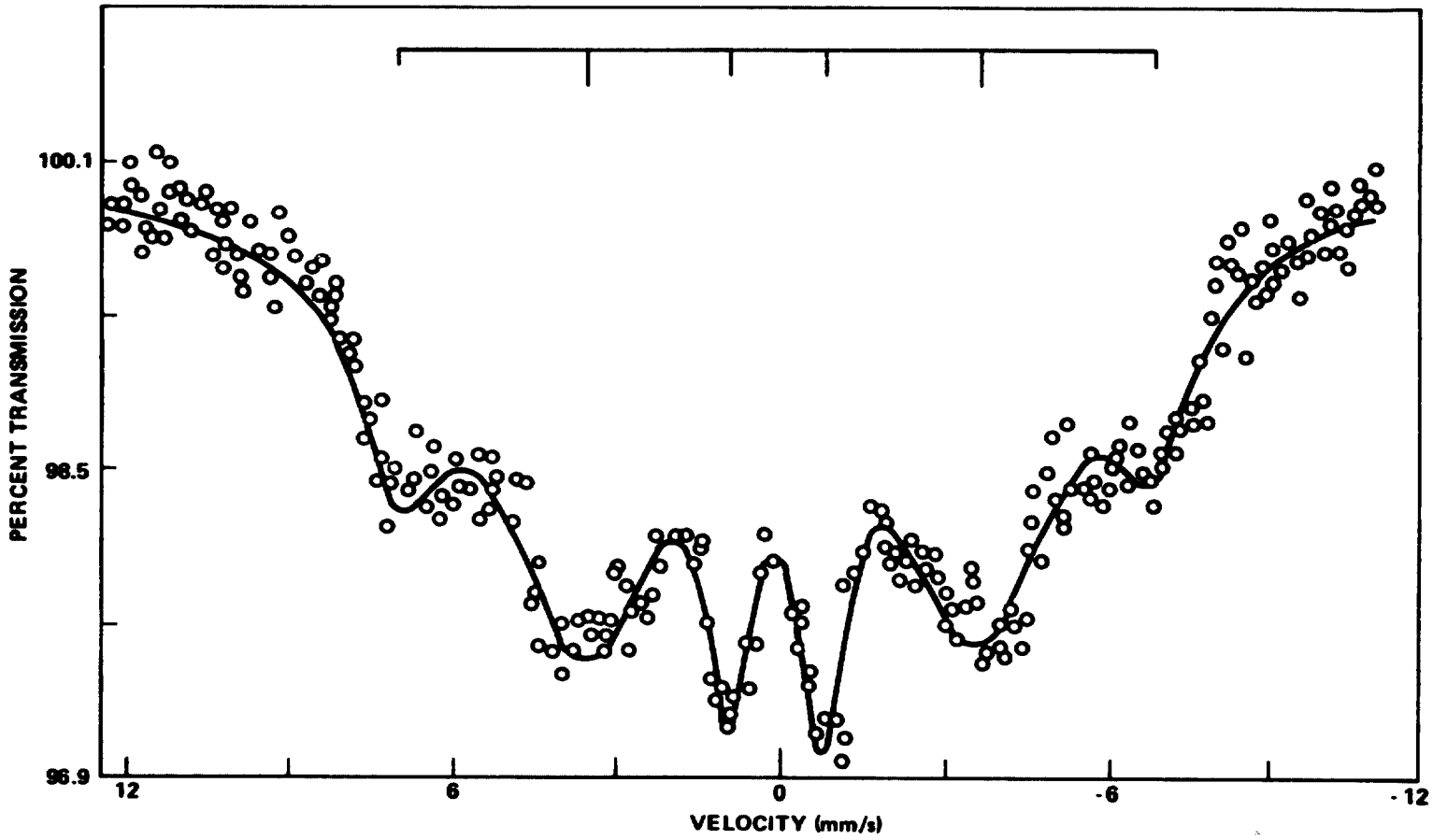

Figure 3. Mössbauer spectrum of $Zn^{2+}_{0.3}Mn^{2+}_{0.7}Mn^{3+}_{0.2}Fe^{3+}_{1.8}O_4$.

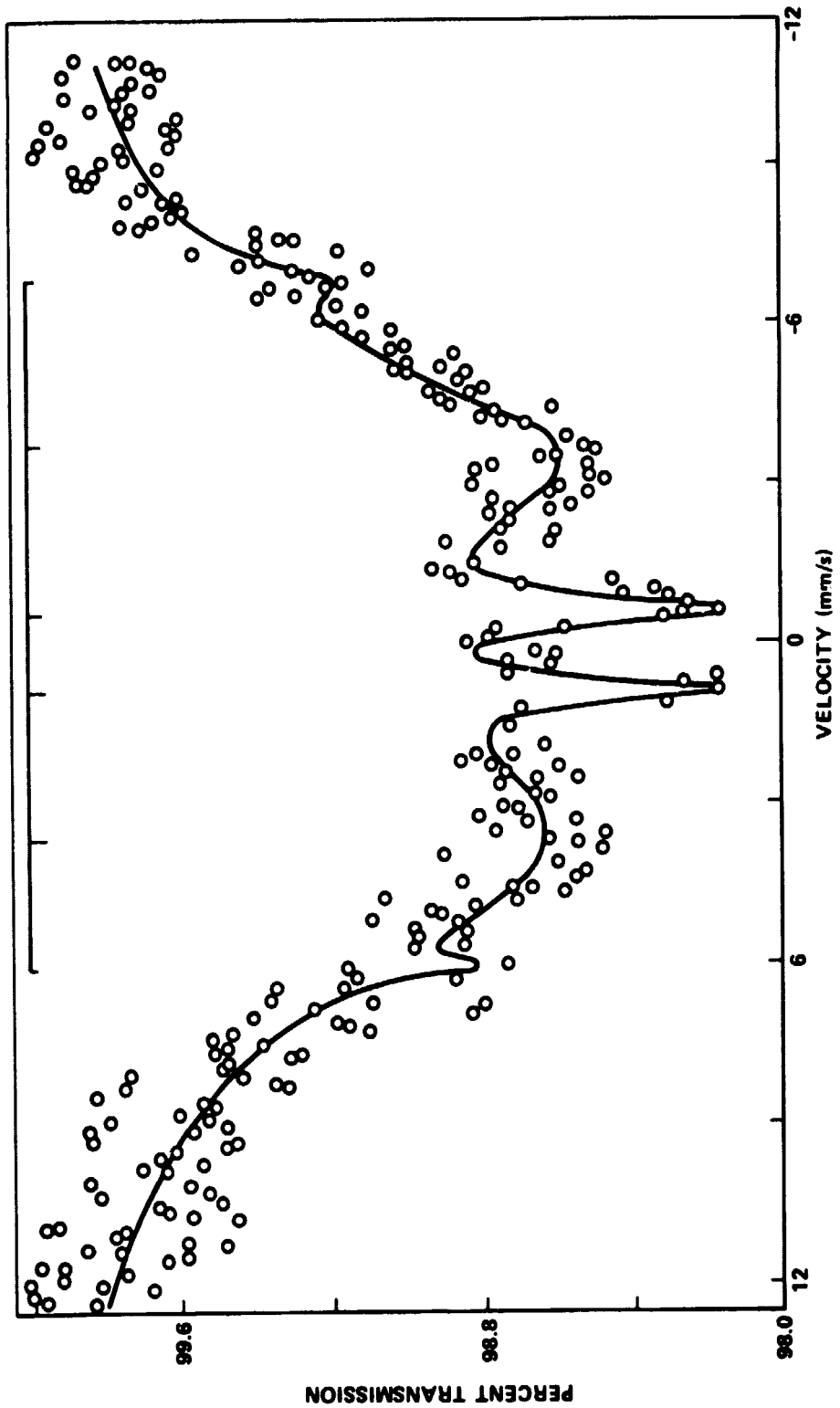

Figure 4. Mössbauer spectrum of $Zn^{2+}_{0.3}Mn^{2+}_{0.7}Mn^{3+}_{0.3}Fe^{3+}_{1.7}O_4$.

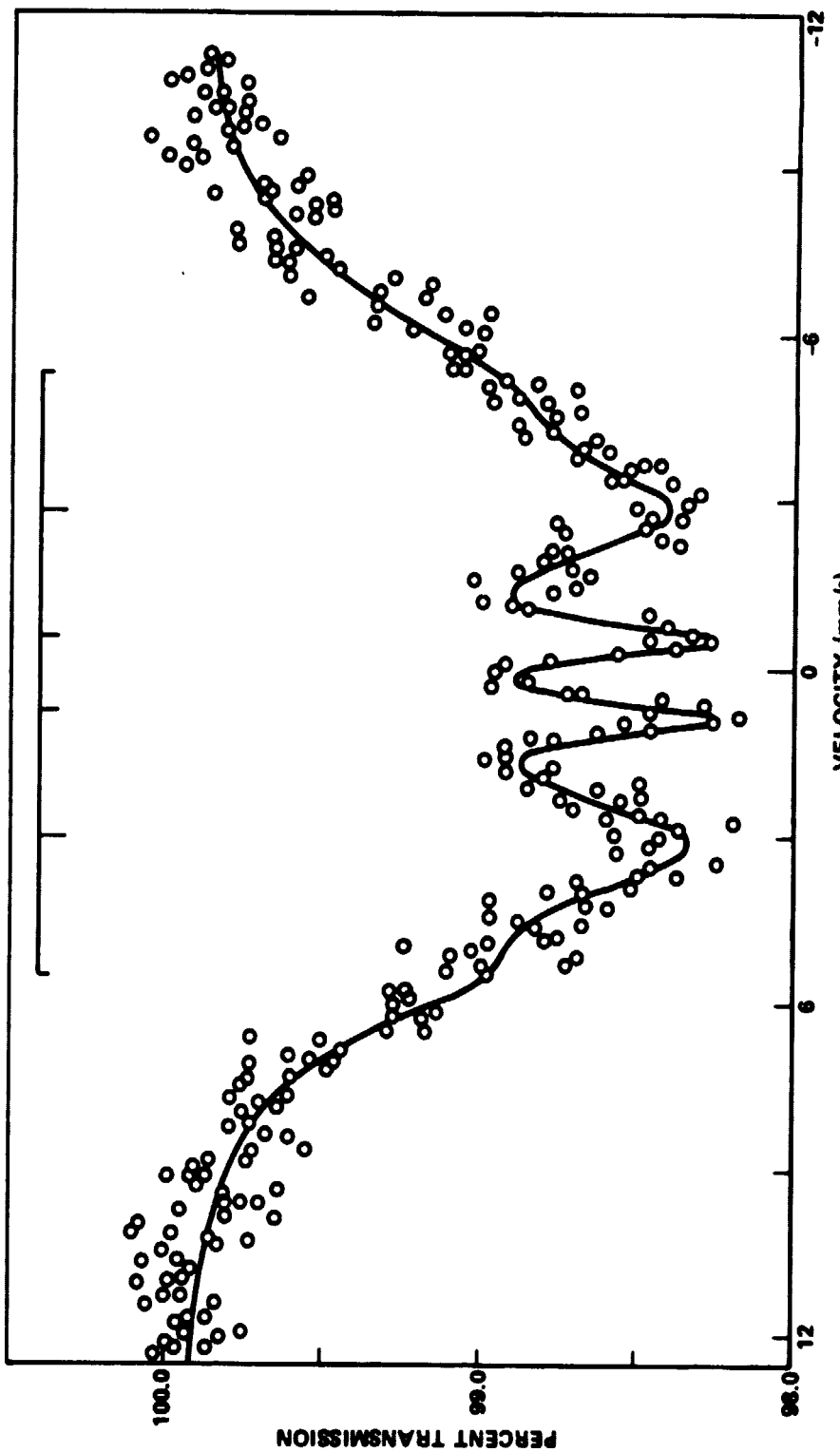

Figure 5. Mössbauer spectrum of $Zn^{2+}_{0.3}Mn^{2+}_{0.7}Mn^{3+}_{0.4}Fe^{3+}_{1.6}O_4$.

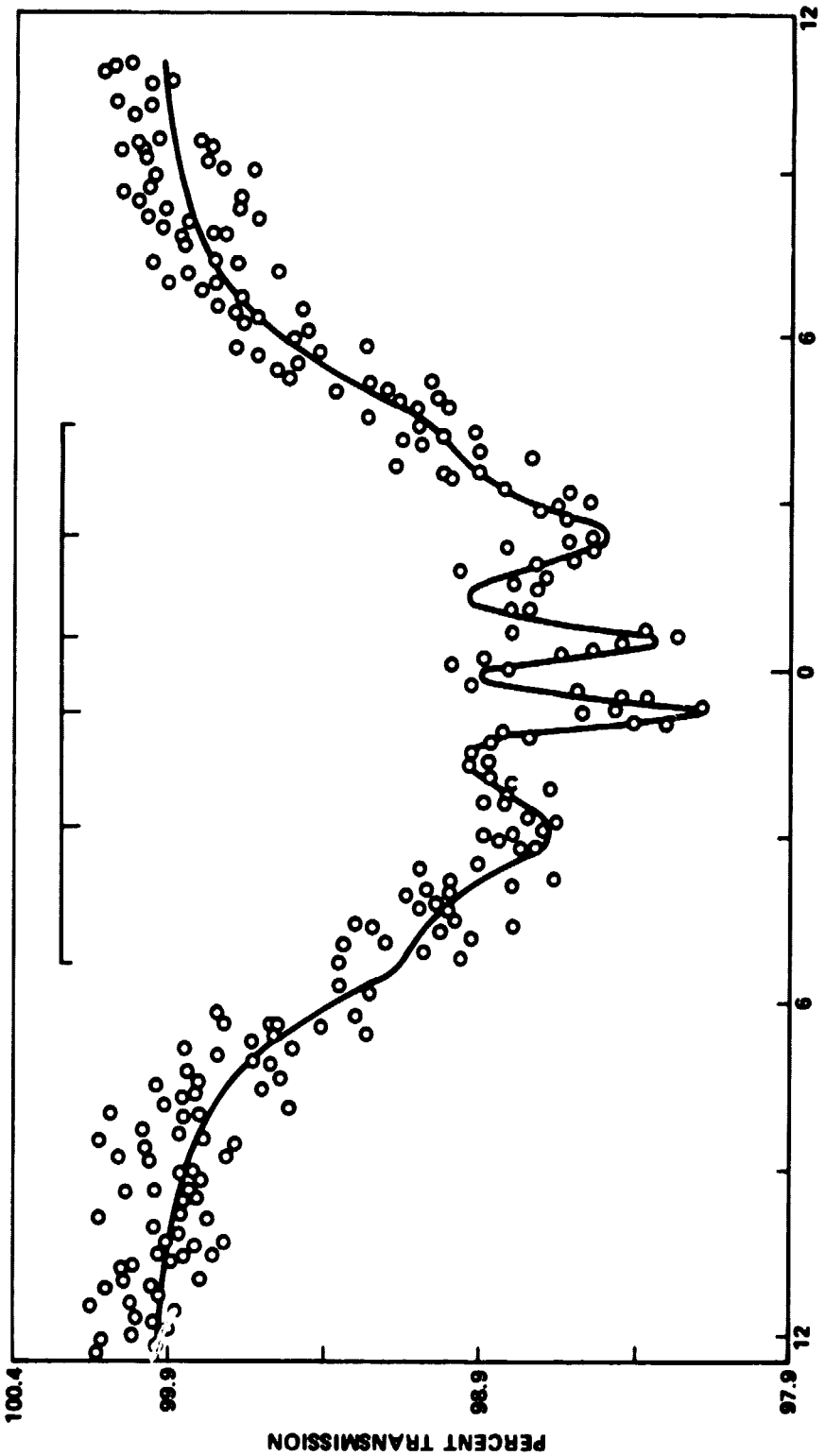

Figure 6. Mössbauer spectrum of $Zn^{2+}_{0.3}Mn^{2+}_{0.7}Mn^{3+}_{0.5}Fe^{3+}_{1.5}O_4$.

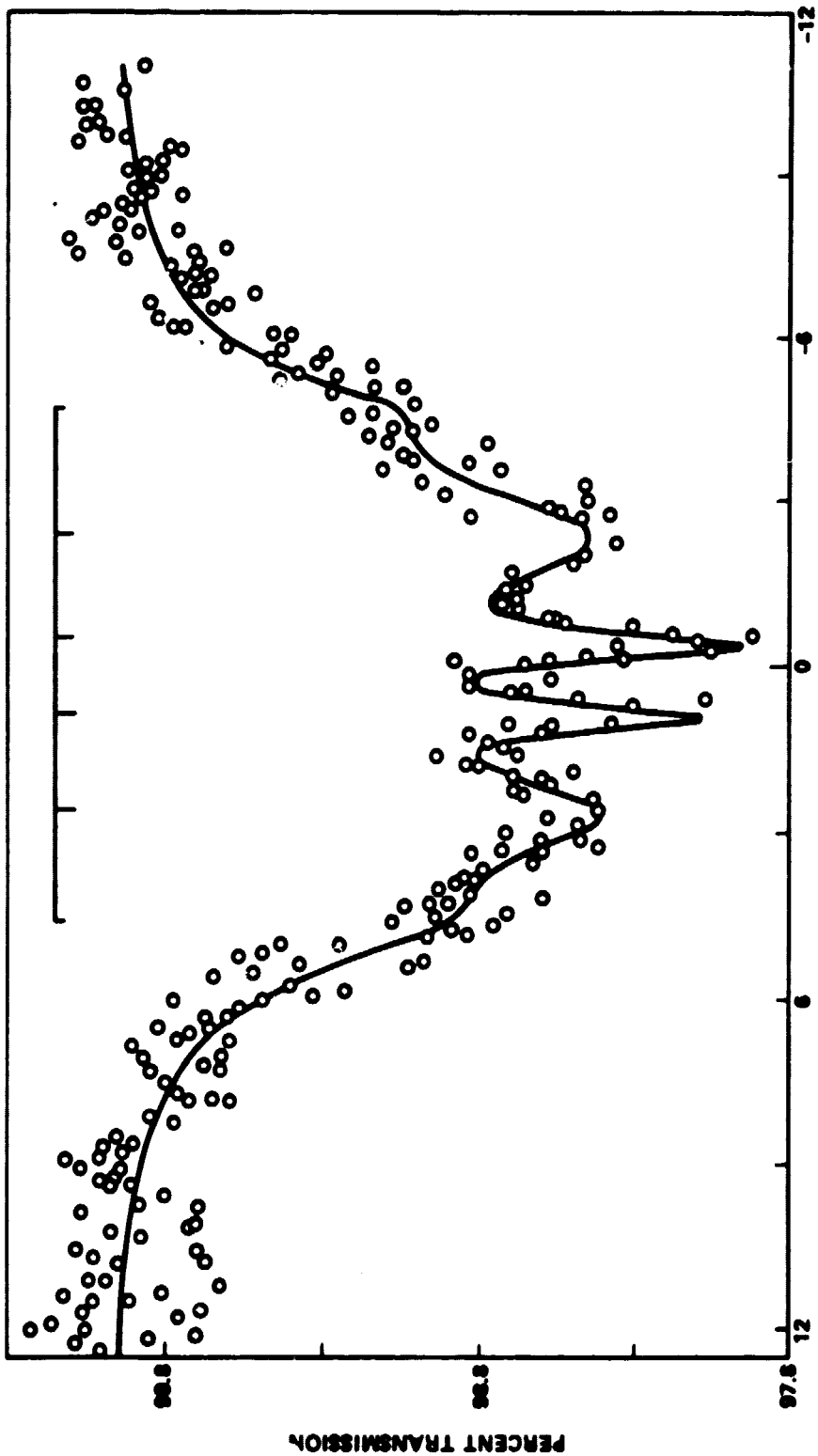

Figure 7. Mössbauer spectrum of $Zn^{2+}_{0.3}Mn^{2+}_{0.7}Mn^{3+}_{0.6}Fe^{3+}_{1.4}O_4$.

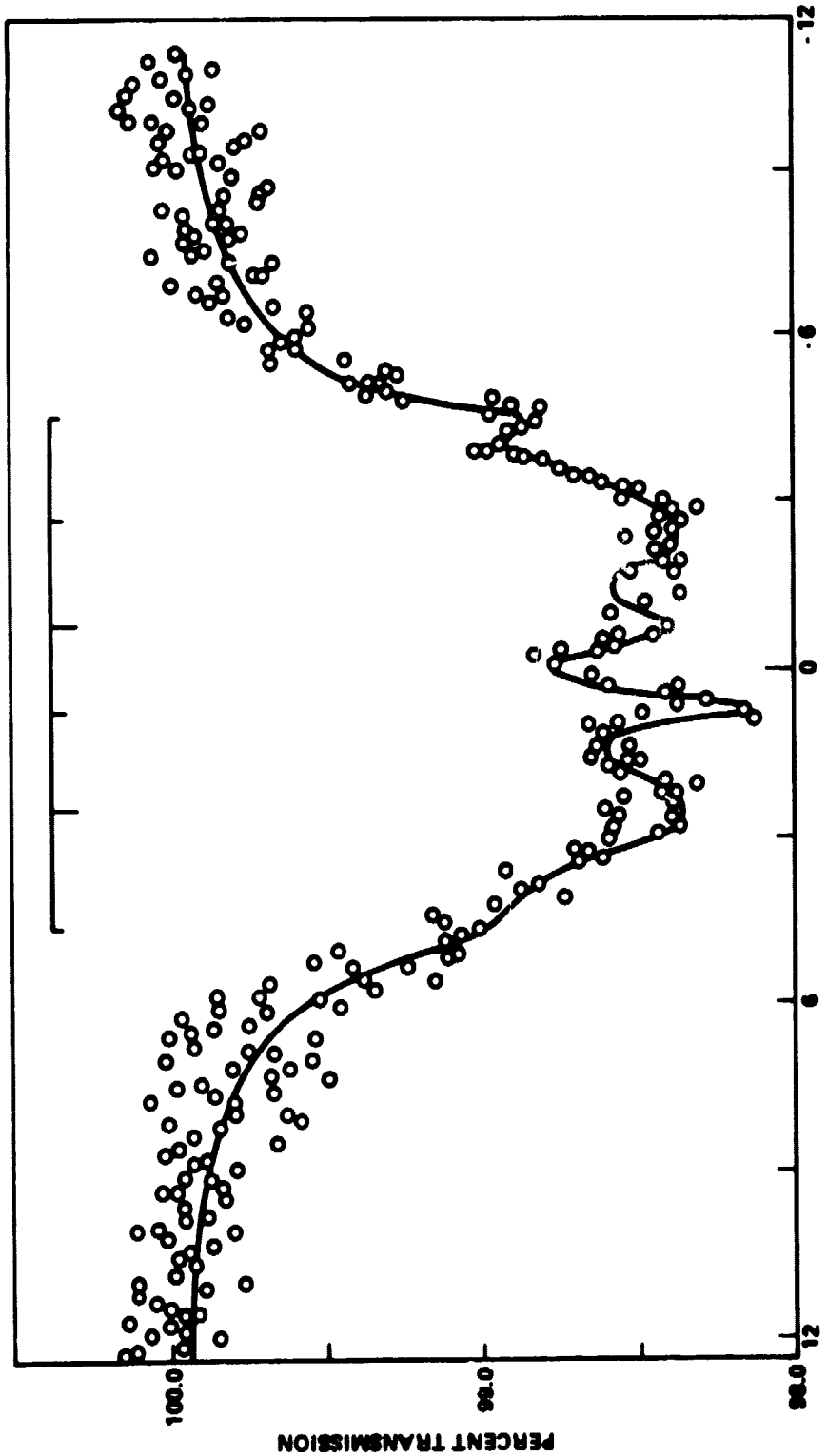

Figure 8. Mössbauer spectrum of $Zn^{2+}_{0.3}Mn^{2+}_{0.7}Mn^{3+}_{0.7}Fe^{3+}_{1.3}O_4$.

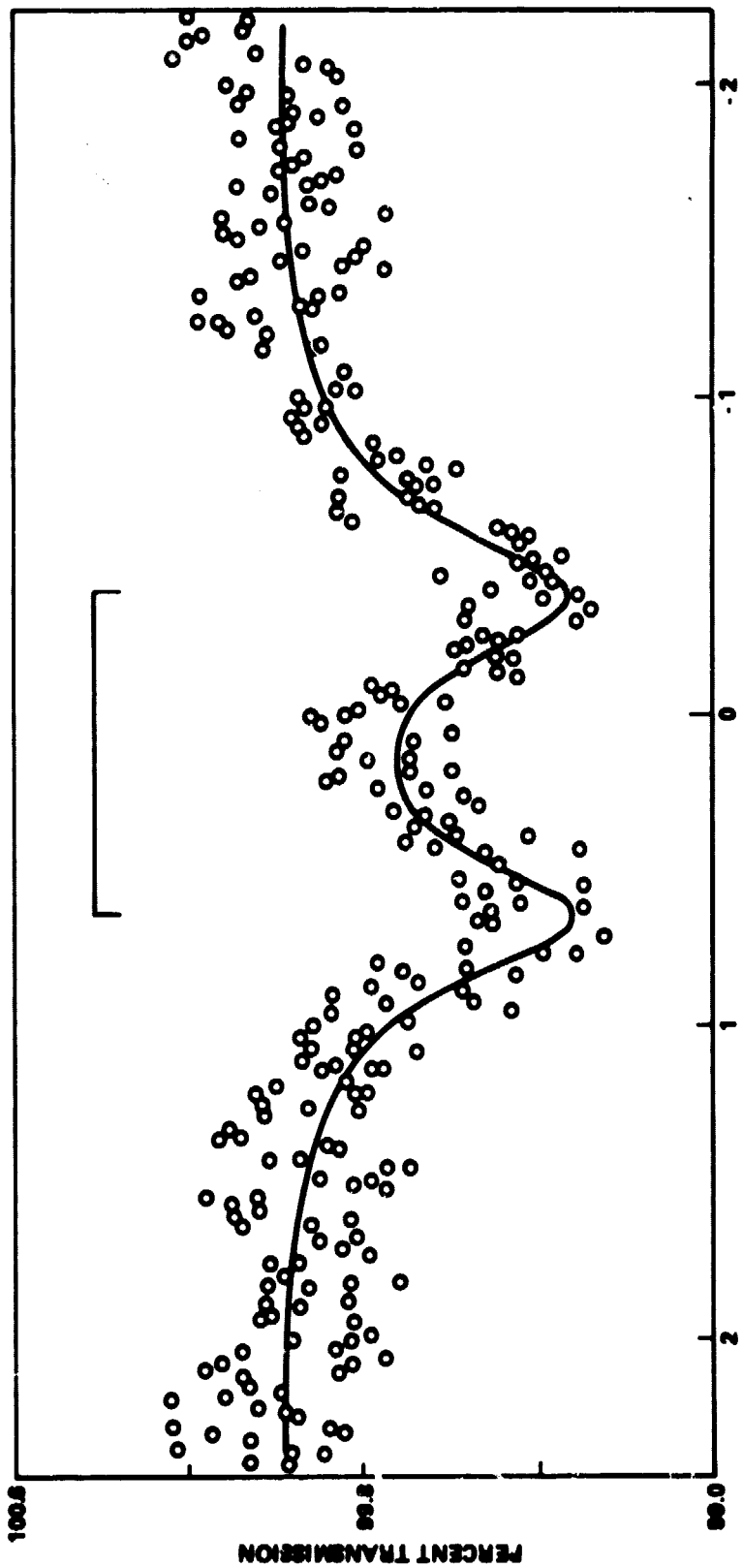

Figure 9. Mössbauer spectrum of $Zn^{2+}_{0.3}Mn^{2+}_{0.7}Mn^{3+}_{0.8}Fe^{3+}_{1.2}O_4$.

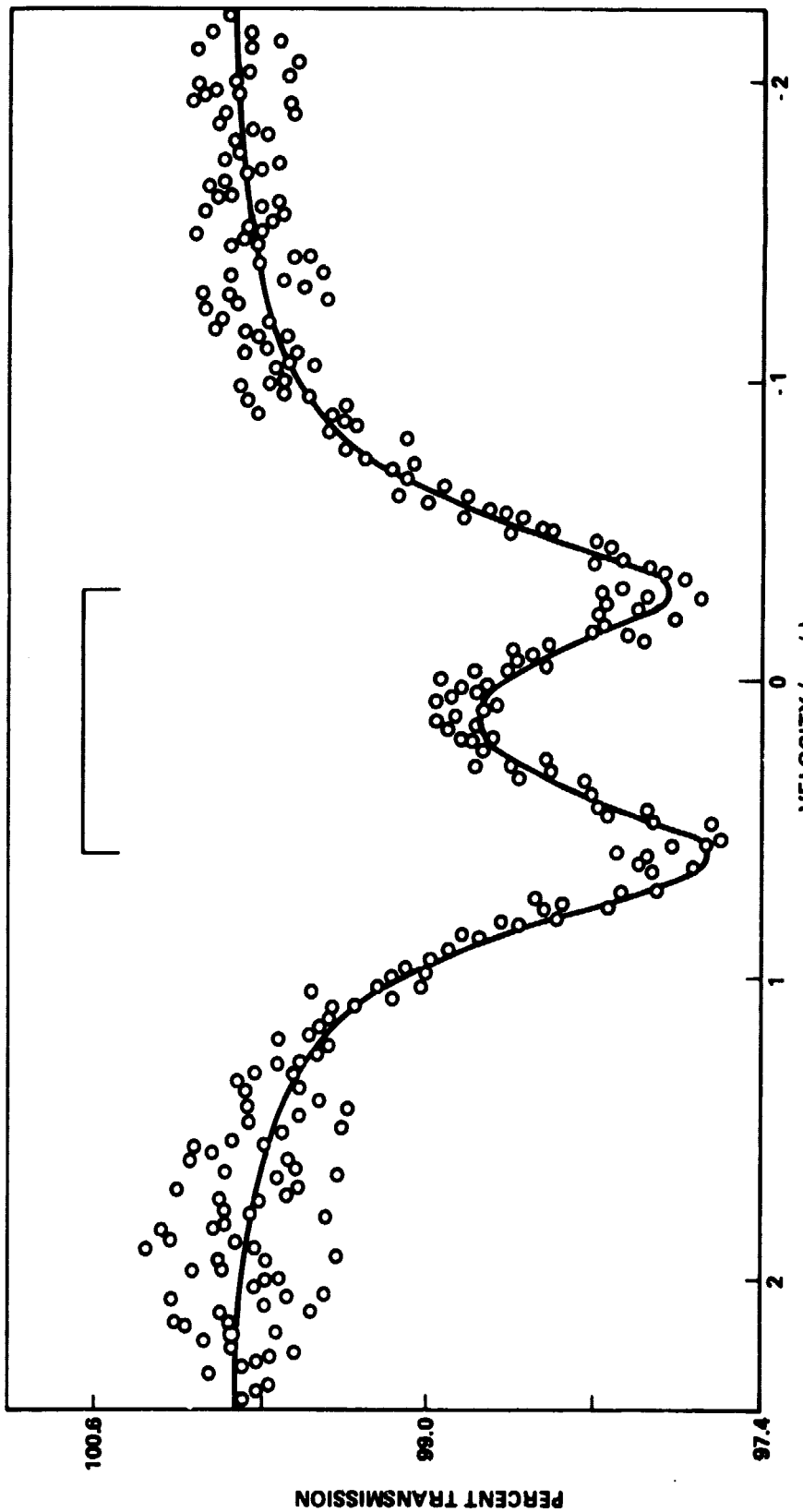

Figure 10. Mössbauer spectrum of $Zn^{2+}_{0.3}Mn^{2+}_{0.7}Mn^{3+}_{0.3}Fe^{3+}_{1.1}O_4$.

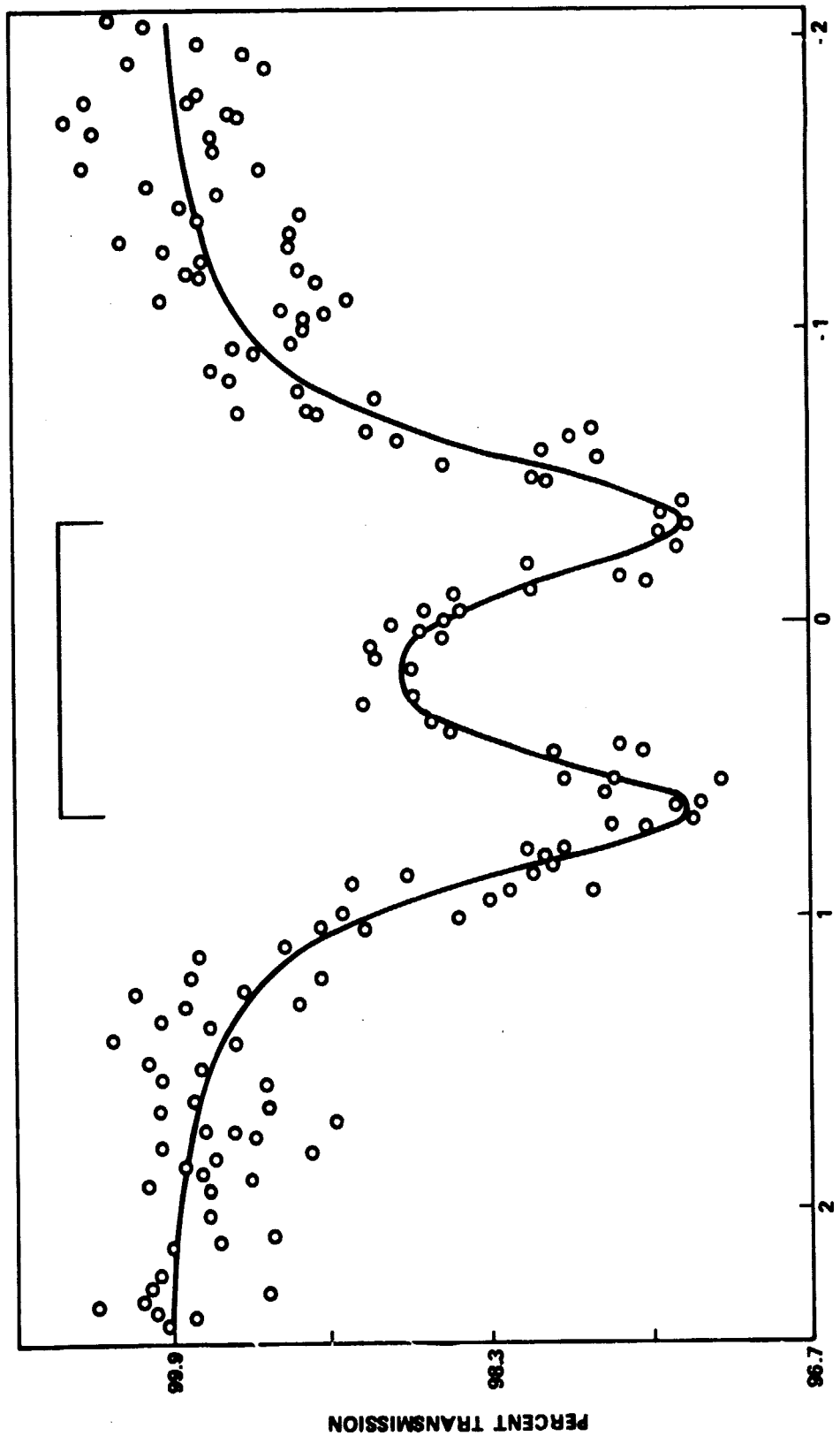

Figure 11. Mössbauer spectrum of $Zn^{2+}_{0.3}Mn^{2+}_{0.7}Mn^{3+}_{1.0}Fe^{3+}_{1.0}O_4$.

REFERENCES

1. Gupta, R. G.; Mendiratta, R. G.; and Escue, W. T.: Mössbauer Studies in Zinc-Manganese Ferrites. NASA TN D.

2. Smith, J. and Wijn, H. P. J.: Ferrites. Philips Technical Library, 1959.

3. Gupta, R. G.: Ph.D. Thesis (Submitted to IIT, Delhi).

4. Neel, L.: Ann. Phys. (Paris), vol. 3, p. 137, 1498.

5. Yafet, Y. and Kittel, C.: Phys. Rev., vol. 87, p. 290, 1952.

6. Kaplan, A.: Phys. Rev., vol. 119, p. 1460, 1960.

7. Anderson, P. W.: Phys. Rev., vol. 102, p. 1008, 1956.

8. Gilleo, M. A.: J. Phys. Chem. Solids, vol. 13, p. 33, 1960.

9. Nowik, I.: J. Appl. Phys., vol. 40, p. 872, 1969.

10. Ishikawa, Y.: J. Phys. Soc. Japan, vol. 17, p. 1835, 1962.

11. Young, J. W.: Ph.D. Dissertation, University of Southern California, 1970.

12. Wickman, H. H. and Wertheim, G. K.: Chemical Application of Mössbauer Spectroscopy, p. 548.

APPROVAL

MÖSSBAUER STUDIES IN $Zn^{2+}_{0.3}\ Mn^{2+}_{0.7}\ Mn^{3+}_{y}\ Fe^{3+}_{2-y}\ O_4$

R. G. Gupta, R. G. Mendiratta, and W. T. Escue

The information in this report has been reviewed for security classification. Review of any information concerning Department of Defense or Atomic Energy Commission programs has been made by the MSFC Security Classification Officer. This report, in its entirety, has been determined to be unclassified.

This document has also been reviewed and approved for technical accuracy.

F. Brooks Moore

F. BROOKS MOORE
Director, Electronics and Control Laboratory

☆ U.S. GOVERNMENT PRINTING OFFICE 1975—641-255/115 REGION NO. 4